Fixed scale approach to equation of state in lattice QCD

PHYSICAL REVIEW D **79,** 051501(R) (2009)

Fixed scale approach to equation of state in lattice QCD

T. Umeda,[1] S. Ejiri,[2] S. Aoki,[1,3] T. Hatsuda,[4] K. Kanaya,[1] Y. Maezawa,[5] and H. Ohno[1]

(WHOT-QCD Collaboration)

[1]*Graduate School of Pure and Applied Sciences, University of Tsukuba, Tsukuba, Ibaraki 305-8571, Japan*
[2]*Physics Department, Brookhaven National Laboratory, Upton, New York 11973, USA*
[3]*RIKEN BNL Research Center, Brookhaven National Laboratory, Upton, New York 11973, USA*
[4]*Department of Physics, The University of Tokyo, Tokyo 113-0033, Japan*
[5]*En'yo Radiation Laboratory, Nishina Accelerator Research Center, RIKEN, Wako, Saitama 351-0198, Japan*

(Received 18 September 2008; published 2 March 2009)

A new approach to study the equation of state in finite-temperature QCD is proposed on the lattice. Unlike the conventional method in which the temporal lattice size N_t is fixed, the temperature T is varied by changing N_t at the fixed lattice scale. The pressure of the hot QCD plasma is calculated by the integration of the trace anomaly with respect to T at the fixed lattice scale. This "T-integral method" is tested in quenched QCD on isotropic and anisotropic lattices and is shown to give reliable results, especially at intermediate and low temperatures.

DOI: 10.1103/PhysRevD.79.051501 PACS numbers: 12.38.Gc, 12.38.Mh

I. INTRODUCTION

The equation of state (EOS) is one of the most fundamental observables to identify different phases in quantum chromodynamics (QCD) at finite temperature T. Also, it is an essential input to describe the space-time evolution of the hot QCD matter created in relativistic heavy ion collisions [1]. So far, lattice QCD is the only systematic method to calculate EOS for a wide range of T across the region of the hadron-quark phase transition (see the recent review, [2]).

Conventionally, the EOS on the lattice is extracted from a method in which $T = (N_t a)^{-1}$ is varied by changing the lattice scale a (or equivalently the lattice gauge coupling $\beta = 6/g^2$) at a fixed temporal lattice size N_t. Using the thermodynamic relation $p = (T/V)\ln Z$, with V being the spatial volume and Z being the partition function, the pressure p is calculated as [3]

$$p = \frac{T}{V}\int_{\beta_0}^{\beta} d\beta \frac{1}{Z}\frac{\partial Z}{\partial \beta} = -\frac{T}{V}\int_{\beta_0}^{\beta} d\beta \left\langle \frac{\partial S}{\partial \beta}\right\rangle. \qquad (1)$$

Here S is the lattice action and $\langle \cdots \rangle$ is the thermal average with a zero-temperature contribution subtracted. (In multiparameter cases such as QCD with dynamical quarks, "β" should be generalized to the position vector in the coupling parameter space [4].) The initial point of integration β_0 is chosen in the low temperature phase from the condition $p(\beta_0) \approx 0$.

In this conventional method, a major part of the computational cost is devoted to zero-temperature simulations; they are necessary to set the lattice scale and to carry out zero-temperature subtractions at the simulation points. Furthermore, for the calculation of the trace anomaly $\epsilon - 3p$, with ϵ being the energy density, the nonperturbative beta functions have to be determined by zero-temperature simulations at the same simulation points. In multiparameter cases, simulations should be performed on a line of constant physics (LCP) in the coupling parameter space in order to identify the effect of temperature on a given physical system. LCP's should be determined also at $T = 0$. These zero-temperature simulations for a wide range of coupling parameters are numerically demanding, in particular, for QCD with dynamical quarks.

In this paper, we push an alternative approach where temperature is varied by N_t with other parameters fixed. The fixed scale approach has been applied with the derivative method [5] in, e.g., Ref. [6]. However, determination of nonperturbative Karsch coefficients for all the simulation points requires quite a bit of work, which will not be easy for QCD with dynamical quarks. Here, we propose a new method, "the T-integral method": To calculate the pressure nonperturbatively, we use

$$\frac{p}{T^4} = \int_{T_0}^{T} dT \frac{\epsilon - 3p}{T^5}, \qquad (2)$$

which is obtained from the thermodynamic relation that is valid at the vanishing chemical potential:

$$T\frac{\partial}{\partial T}\left(\frac{p}{T^4}\right) = \frac{\epsilon - 3p}{T^4}. \qquad (3)$$

The initial temperature T_0 is chosen such that $p(T_0) \approx 0$. Calculation of $\epsilon - 3p$ requires the beta functions just at the simulation point, but no further Karsch coefficients are necessary. Since T is restricted to have discrete values, we need to make an interpolation of $(\epsilon - 3p)/T^4$ with respect to T.

Since the coupling parameters are common to all temperatures, our fixed scale approach with the T-integral method has several advantages over the conventional approach: (i) $T = 0$ subtractions can be done by a common

zero-temperature simulation, (ii) the condition to follow the LCP is obviously satisfied, and (iii) the lattice scale as well as beta functions are required only at the simulation point. As a result of these conditions, the computational cost needed for $T = 0$ simulations is largely reduced. We may even borrow results of existing high precision spectrum studies at $T = 0$, which are publicly available e.g. on the International Lattice Data Grid [7]. On the other hand, when the beta functions are not available, we need to perform additional $T = 0$ simulations around the simulation points, as in the case of the conventional method.

For a continuum extrapolation, we need to repeat the calculation at a couple of lattice spacings. If we adopt coupling parameters from $T = 0$ spectrum studies in which the continuum extrapolation has already been performed, we can get all the configurations for $T = 0$ subtractions. Furthermore, because the lattice spacings in spectrum studies are usually smaller than those used in conventional fixed-N_t studies around the critical temperature T_c, the values of N_t in our approach are much larger there than those in conventional studies. For example, at $a \approx 0.07$ fm, $T \sim 175$ MeV is achieved by $N_t \sim 16$. Therefore, for thermodynamic quantities around T_c, we can largely reduce the lattice artifacts due to large a and/or small N_t over the conventional approach, without high computational costs for $T = 0$ calculations. This is also good news for phenomenological applications of the EOS, since the temperature achieved in the relativistic heavy ion collisions at the Relativistic Heavy Ion Collider and the LHC will be, at most, up to a few times the critical temperature [1]. On the other hand, calculation of the trace anomaly around and below T_c with large values of N_t may require high statistics due to large cancellations by the $T = 0$ subtraction. We note here that, as T increases, N_t becomes small and hence the lattice artifact increases. Therefore, our approach is not suitable for studying how the EOS approaches the Stephan-Boltzmann value in the high T limit.

The outline of this paper is as follows. After introducing our lattice action and the trace anomaly in Sec. II, we test our T-integral method in SU(3) gauge theory on an isotropic lattice in Sec. III and on an anisotropic lattice in Sec. IV. The last section is devoted to a summary and conclusions.

II. LATTICE ACTION

We study SU(3) gauge theory with the standard plaquette gauge action on isotropic and anisotropic lattices with the spatial (temporal) lattice size N_s (N_t) and lattice spacing a_s (a_t). The lattice action is given by

$$S = \beta\xi_0 \sum_x \sum_{i=1}^{3} \left[1 - \frac{1}{3} \mathrm{Re\,Tr} U_{i4}(x) \right] + \frac{\beta}{\xi_0} \sum_x \sum_{i>j=1}^{3} \left[1 - \frac{1}{3} \mathrm{Re\,Tr} U_{ij}(x) \right] \tag{4}$$

$$\stackrel{\text{def.}}{=} 3N_s^3 N_t \beta \{ \xi_0 P_t + \xi_0^{-1} P_s \} \tag{5}$$

where $U_{\mu\nu}(x)$ is the plaquette in the $\mu\nu$ plane and β and ξ_0 are the bare lattice gauge coupling and bare anisotropy parameters. The trace anomaly is obtained as

$$\frac{\epsilon - 3p}{T^4} = \frac{N_t^3}{N_s^3 \xi^3} a_s \left(\frac{\partial \beta}{\partial a_s} \right)_\xi \left\langle \left(\frac{\partial S}{\partial \beta} \right)_\xi \right\rangle \tag{6}$$

$$= \frac{3N_t^4}{\xi^3} \left\langle \left(a_s \frac{\partial \beta}{\partial a_s} \right)_\xi \left[\left\{ \frac{1}{\xi_0} P_s + \xi_0 P_t \right\} - \frac{\beta}{\xi_0} \left(\frac{\partial \xi_0}{\partial \beta} \right)_\xi \left\{ \frac{1}{\xi_0} P_s - \xi_0 P_t \right\} \right] \right\rangle \tag{7}$$

where $\xi = a_s/a_t$ is the renormalized anisotropy and $a_s(\partial\beta/\partial a_s)_\xi$ is the beta function. Note that $(\partial\xi_0/\partial\beta)_\xi = 0$ on isotropic lattices.

III. EOS ON AN ISOTROPIC LATTICE

Our simulation parameters are listed in Table I. We calculate the EOS on three isotropic lattices to study the volume and lattice spacing dependence. The ranges of N_t correspond to $T = 210$–700 MeV for the sets i1 and i2, and $T = 220$–730 MeV for i3. The critical temperature corresponds to $N_t \sim 7$–8 for i1 and i2, and ~ 10 for i3, assuming $T_c \sim 290$ MeV in quenched QCD with the Sommer scale $r_0 = 0.5$ fm. Set a2 will be discussed in the next section. The zero-temperature subtraction is performed with $N_t = 16$ for i1 and i2, and with $N_t = 22$ for i3. We generate up to a few million configurations using the pseudo-heat-bath algorithm. Statistical errors are estimated using the jackknife analysis. Typically, bin sizes of a few thousand configurations are necessary near T_c, while a few hundred are sufficient off the transition region.

Figure 1 shows $(\epsilon - 3p)/T^4$. Dotted lines in the figure are the natural cubic spline interpolations. For comparison, we also reproduce the result of the fixed N_t method at $N_t = 8$ and $N_s = 32$ [9], for which we have rescaled the horizontal axis by $T_c = 290$ MeV according to our choice of $r_0 = 0.5$ fm. At and below T_c, lattice size dependence is visible among sets i1 ($L \approx 1.5$ fm) and i2 (2.2 fm) and the fixed $N_t = 8$ result (2.7 fm). On the other hand, the lattice spacing dependence is negligible between i1 ($a \approx 0.093$ fm) and i3 (0.068 fm). At higher T, $(\epsilon - 3p)/T^4$

TABLE I. Simulation parameters on isotropic and anisotropic lattices. On isotropic lattices, we adopt the r_0/a of [8] and the beta function of [9]. The anisotropy r_0/a_s is from [10], while the beta function is calculated in Sec. IV. The lattice scale a_s and lattice size $L = N_s a_s$ are calculated with $r_0 = 0.5$ fm.

Set	β	ξ	N_s	N_t	r_0/a_s	a_s(fm)	L(fm)	$a(dg^{-2}/da)$
i1	6.0	1	16	3–10	$5.35(^{+2}_{-3})$	0.093	1.5	−0.098 172
i2	6.0	1	24	3–10	$5.35(^{+2}_{-3})$	0.093	2.2	−0.098 172
i3	6.2	1	22	4–13	7.37(3)	0.068	1.5	−0.112 127
a2	6.1	4	20	8–34	5.140(32)	0.097	1.9	−0.107 04

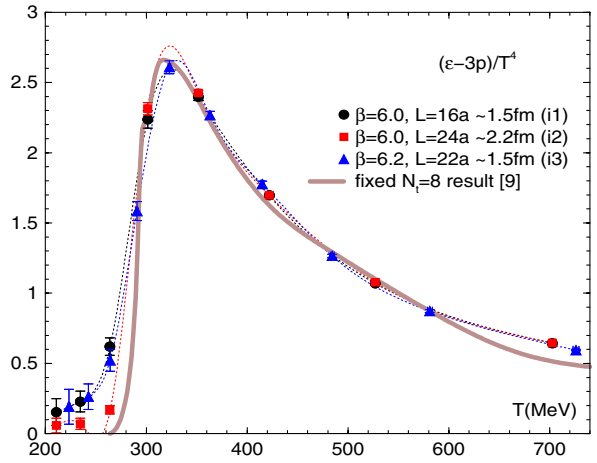

FIG. 1 (color online). Trace anomaly on isotropic lattices as a function of physical temperature. The dotted lines are natural cubic spline interpolations. Horizontal errors due to the lattice scale are smaller than the symbols.

on our three lattices show good agreement; however, they slightly deviate from the fixed N_t one at $T > 600$ MeV, presumably due to the coarseness of our lattices at these temperatures.

The integration of (2) is performed numerically using the natural cubic spline interpolations shown in Fig. 1. For the initial temperature T_0 of the integration, we linearly extrapolate the $(\epsilon - 3p)/T^4$ data at the few lowest T's because the values of $(\epsilon - 3p)/T^4$ at our lowest T are not exactly zero. In this study, we commonly take $T_0 = 150$ MeV as the initial temperature which satisfies $(\epsilon - 3p)/T^4 = 0$, and estimate the integration from T_0 to the lowest T by the area of the triangle.

We estimate the statistical error for the T integration by the jackknife analysis at each T and accumulate the contributions from different T's by the error propagation [11], because simulations at different N_t are statistically independent. Note that the error for the lattice scale does not affect the dimensionless quantity p/T^4. Error bars shown in the figures represent the statistical errors.

To estimate the systematic error due to the interpolation ansatz, we compare the results of p/T^4 using cubic spline interpolation and those with the trapezoidal rule in Fig. 2. (The results on the anisotropic $\xi = 4$ lattice will be discussed later.) We find that the size of systematic errors due to the interpolation ansatz is comparable to that of the statistical ones. In Fig. 3, we note that the natural cubic spline interpolation curve of $(\epsilon - 3p)/T^4$ for set i2 shows small negative values at $T \approx 250$ MeV due to the nearby sharp edge at $T \approx 260$ MeV. From a comparison with the results of trapezoidal interpolation for that range, we find that the effect of this bump on the value of p/T^4 at $T > 250$ MeV is 0.032. Although a negative pressure is unphysical, because this shift in p/T^4 is smaller than the statistical errors, we disregard the effects of the negative pressure in this paper. To avoid arbitrary data handling, we just adopt the results of natural cubic spline interpolations as the central values in the following.

In Fig. 3, we summarize the results of the EOS. Results on the anisotropic lattice (a2) will be discussed later. The normalized energy density ϵ/T^4 is calculated by combining p/T^4 and $(\epsilon - 3p)/T^4$.

We find that, except for the vicinity of T_c, the EOS is rather insensitive to the variation of lattice size (between $L \approx 1.5$ fm and 2.2 fm) and lattice spacing (between $a \approx 0.093$ fm and 0.063 fm). The results of the EOS agree within 10% for our variation of lattice parameters. This is in part due to the fact that $(\epsilon - 3p)/T^4$ is not so sensitive to the lattice parameters up to high temperatures. Note also that, because $(\epsilon - 3p)/T^4 = 0$ in the high temperature limit, the increasingly large lattice artifacts at large T are naturally suppressed in the T integration. Looking more closely at the $T \gtrsim T_c$ region, we note that both p and ϵ have a slight tendency to decrease as the lattice size (lattice spacing) becomes larger (smaller).

Near and below T_c, we observe a sizable finite size effect between $L \approx 1.5$ fm (i1) and 2.2 fm (i2), while the effect

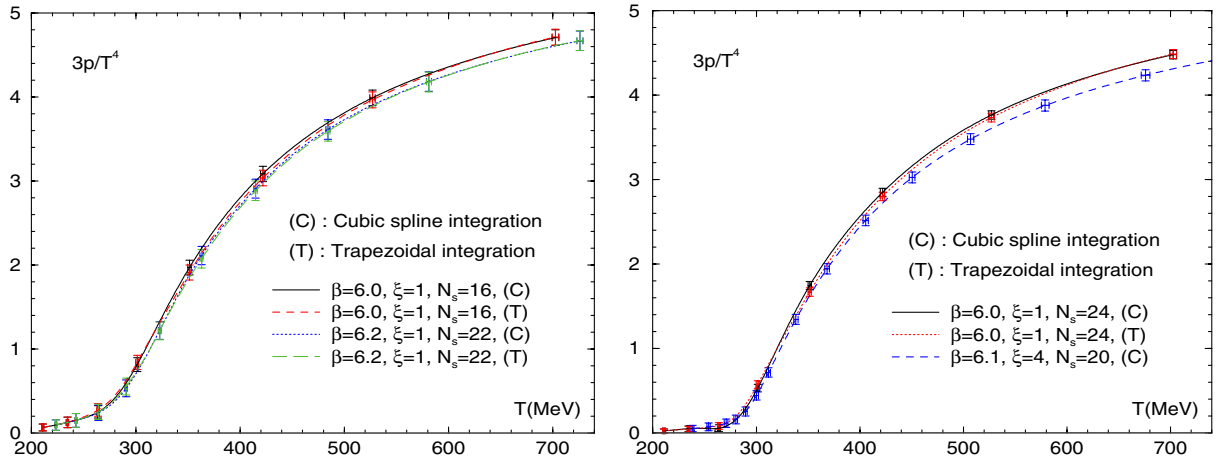

FIG. 2 (color online). Comparison of the pressure using different interpolation functions for integration. Statistical errors are estimated using the jackknife method [11].

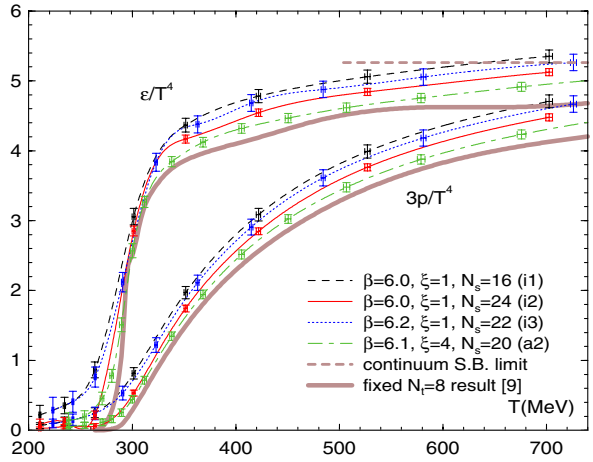

FIG. 3 (color online). The EOS on isotropic and anisotropic lattices. The dashed horizontal line represents the free gas case in the continuum (Stefan-Boltzmann limit).

of the lattice spacing is quite small (i1 and i3). Therefore, for a reliable simulation, we need, at least, $L \gtrsim 2$ fm.

Our results are qualitatively consistent with the previous EOS by the fixed N_t method [9]. Quantitatively, our results are slightly above the fixed N_t results. The discrepancy can be understood in part by smaller spatial volumes below T_c and the small values of N_t at higher T in our method.

IV. THE EOS ON AN ANISOTROPIC LATTICE

An anisotropic lattice with a temporal lattice finer than the spatial one is expected to improve the resolution of T without increasing the computational cost much. To further test the systematic error due to the resolution of T, we perform the study using the T-integral method on an anisotropic lattice with the renormalized anisotropy $\xi = 4$.

The simulation parameters are given as set a2 in Table I, which are the same as those adopted in [10]. We vary $N_t = 34 - 8$ corresponding to $T = 240$–1010 MeV. The zero-temperature subtraction is performed with $N_t = 80$. ($= 20 \times \xi$). We generate up to a few million configurations.

We calculate the beta function $a_s(\partial\beta/\partial a_s)_\xi$ by fitting the r_0/a_s data [10,12] with Allton's ansatz [13].

$$a_s/r_0 = R(\beta) \cdot A(1 + B\hat{f}^2(\beta) + C\hat{f}^4(\beta)), \qquad (8)$$

where

$$R(\beta) = \left(\frac{6b_0}{\beta}\right)^{-b_1/(2b_0^2)} \exp\left(-\frac{\beta}{12b_0}\right),$$

$$\hat{f}(\beta) = R(\beta)/R(6.10), \qquad b_0 = \frac{11}{16\pi^2},$$

$$b_1 = \frac{102}{(16\pi^2)^2}.$$

The best fit is achieved by $A = 76.0(1.5)$, $B = 0.190(32)$, and $C = 0.0204(87)$ with $\chi^2/\mathrm{dof} = 12.6/6$. The beta function is now obtained by

$$a_s\left(\frac{\partial\beta}{\partial a_s}\right)_\xi = \frac{12b_0^2\beta}{6b_1 - b_0\beta} \frac{1 + B\hat{f}^2 + C\hat{f}^4}{1 + 3B\hat{f}^2 + 5C\hat{f}^4}, \qquad (9)$$

and its value at our simulation point is given in Table I. For $(\partial\xi_0/\partial\beta)_\xi$ we adopt the result of [14].

In Fig. 4, we compare the trace anomaly obtained on the anisotropic lattice with that on the isotropic lattice with similar a_s and L (set i2). We find that the results are generally consistent with each other, while, due to the cruder resolution in T, the natural cubic spline interpolation for the i2 lattice slightly overshoots the data on the a2 lattice around the peak at $T \approx 320$ MeV. We note that the height of the peak on the a2 lattice is similar to that of the fine i3 lattice shown in Fig. 1 as well as the fixed $N_t = 8$ result. Similar to the case of the isotropic lattice, our result slightly overshoots the fixed N_t result below T_c and at $T >$ 600 MeV. Around the sharp lower edge at $T \approx 250$ MeV, the undershooting of the natural cubic spline interpolation on the i2 lattice, discussed in the previous section, is avoided by the finer data points on the a2 lattice.

The results of pressure on the a2 and i2 lattices are compared in the lower panel of Fig. 2. While they are roughly consistent with each other, we find that the pressure on the anisotropic lattice is slightly smaller than that on the isotropic lattice. This is in part due to the smaller values of $\epsilon - 3p$ around the peak at $T \approx 320$ MeV. We also note that the trace anomaly on the a2 lattice has a slight tendency to be systematically lower than that on the i2 lattice by about 1σ on the high temperature side.

When we consider the difference between the a2 and i2 lattices as the systematic error due to the cruder T resolution of the i2 lattice, the systematic error is about 2–3 times larger than the estimation in the previous section from a comparison of different interpolation ansätze. Therefore, for an estimation of the systematic error on isotropic lattices, it may be safer to assume errors a few times larger than those estimated from a comparison of different interpolation ansätze.

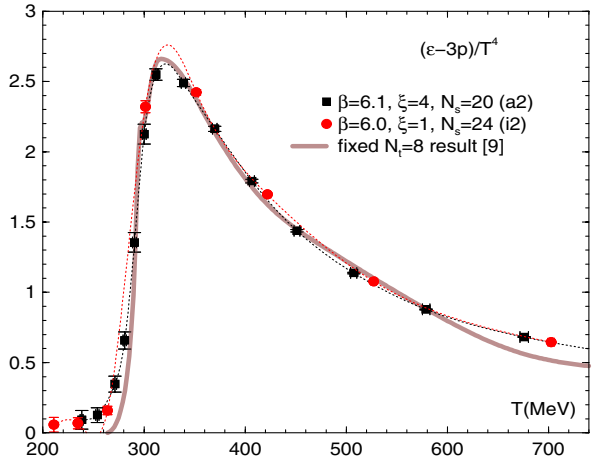

FIG. 4 (color online). Trace anomaly on isotropic and anisotropic lattices with similar spatial lattice spacing and lattice size. The dotted lines are natural cubic spline interpolations.

Some part of this difference in the EOS between a2 and i2 lattices might be explained by the difference of the lattice spacing in the temporal direction, since lattice artifacts of thermodynamic quantities generally have dominant contributions from the temporal lattice spacing [15]. Indeed, this interpretation is supplemented by the fact that the difference in the EOS between i1 and i3 has a similar tendency, as shown in Fig. 3. We reserve further investigation of this possibility for future study.

V. CONCLUSIONS

We proposed a fixed scale approach to investigate finite-temperature QCD on the lattice. To calculate the EOS nonperturbatively at a fixed scale, we introduced the T-integral formula (2), in which p is calculated as an integration of the trace anomaly $\epsilon - 3p$ with respect to T. The fixed scale approach using the T-integral method enables us to efficiently utilize the results of previous $T = 0$ spectrum studies. At intermediate and low temperatures, we can largely reduce the lattice artifacts compared to the fixed N_t approach. On the other hand, our approach is not suitable for studying the approach to the high T limit because of the small N_t there. Also, around and below T_c, the large values of N_t may require high statistics due to large cancellations by the $T = 0$ subtraction.

To test the T-integral method, we performed a series of simulations of SU(3) gauge theory on isotropic and anisotropic lattices. We found that the method works quite well. Our results of the EOS for the quenched QCD on isotropic and anisotropic lattices are summarized in Fig. 3, and are qualitatively consistent with the previous results using the conventional fixed N_t approach.

Our EOS in the high temperature region turned out to be roughly independent of the lattice spacing, lattice volume, and anisotropy. All the results agree within about 10% for the range of our lattice parameters. With small statistical errors of less than about 2%, we identified small systematic shifts under the variations of lattice parameters. Their smallness will be useful for precise continuum extrapolations. Around the critical temperature, we found that the lattice size should be at least larger than about 2 fm.

The fixed scale approach using the T-integral method is applicable to QCD with dynamical quarks too. With dynamical quarks, it is more convenient to simulate isotropic lattices, because the tuning of anisotropy parameters, as well as the determination of the factors $\partial\xi_0/\partial\beta$ in (7), requires quite a bit of work for full QCD. Therefore, it is important to estimate the systematic error in the EOS due to the limited resolution of T on an isotropic lattice. From the test of quenched QCD presented in this paper, we found that this systematic error is under control and its order of magnitude can be correctly estimated by a comparison of different interpolation ansätze, though it may be safer to introduce a factor of about 2–3 to the estimates.

We are currently investigating the EOS in $2 + 1$ flavor QCD with nonperturbatively improved Wilson quarks, using the configurations by the CP-PACS/JLQCD Collaboration [16], which are publicly available on the International Lattice Data Grid [7]. The pseudocritical temperature (~ 175 MeV) is around $N_t \sim 16$ on the finest lattice with $a \approx 0.07$ fm. We are further planning to extend the study to use the $2 + 1$ flavor configurations by the PACS-CS Collaboration generated just at the physical values of the light quark masses [17].

ACKNOWLEDGMENTS

T. U. thanks H. Matsufuru for helpful discussions and for r_0/a_s data on the anisotropic lattice. The simulations have been performed on supercomputers at RCNP, Osaka University and YITP, Kyoto University. This work is in part supported by Grants-in-Aid of the Japanese Ministry of Education, Culture, Sports, Science and Technology (No. 17340066, No. 18540253, No. 19549001, and No. 20340047). S. E. is supported by the U.S. Department of Energy (No. DE-AC02-98CH10886).

[1] T. Hirano, N. van der Kolk, and A. Bilandzic, arXiv:0808.2684.
[2] C. DeTar, Proc. Sci., LAT2008 (2008) 001.
[3] J. Engels, J. Fingberg, F. Karsch, D. Miller, and M. Weber, Phys. Lett. B **252**, 625 (1990).
[4] A. Ali Khan *et al.* (CP-PACS Collaboration), Phys. Rev. D **64**, 074510 (2001).
[5] J. Engels, F. Karsch, H. Satz, and I. Montvay, Phys. Lett. **101B**, 89 (1981).
[6] L. Levkova, T. Manke, and R. Mawhinney, Phys. Rev. D **73**, 074504 (2006).
[7] T. Yoshié, Proc. Sci., LAT2008 (2008) 019.
[8] R. G. Edwards, U. M. Heller, and T. R. Klassen, Nucl. Phys. **B517**, 377 (1998).
[9] G. Boyd *et al.*, Nucl. Phys. **B469**, 419 (1996).
[10] H. Matsufuru, T. Onogi, and T. Umeda, Phys. Rev. D **64**, 114503 (2001).
[11] M. Okamoto *et al.* (CP-PACS Collaboration), Phys. Rev. D **60**, 094510 (1999).
[12] H. Matsufuru (private communication).
[13] C. R. Allton, Nucl. Phys. B, Proc. Suppl. **53**, 867 (1997).
[14] T. R. Klassen, Nucl. Phys. **B533**, 557 (1998).
[15] Y. Namekawa *et al.* (CP-PACS Collaboration), Phys. Rev. D **64**, 074507 (2001).
[16] T. Ishikawa *et al.* (CP-PACS/JLQCD Collaborations), Phys. Rev. D **78**, 011502(R) (2008).
[17] Y. Kuramashi, Proc. Sci., LAT2008 (2008) 018.